Volume 18
Number 11
21 March 2020
Pages 2005-2184

Organic & Biomolecular Chemistry

rsc.li/obc

ISSN 1477-0520

ROYAL SOCIETY OF CHEMISTRY

PAPER

Joshua P. Barham *et al.*

Base-catalyzed C-alkylation of potassium enolates with styrenes *via* a metal–ene reaction: a mechanistic study

Organic & Biomolecular Chemistry

ROYAL SOCIETY OF CHEMISTRY

PAPER

View Article Online
View Journal | View Issue

Cite this: *Org. Biomol. Chem.*, 2020, **18**, 2063

Base-catalyzed C-alkylation of potassium enolates with styrenes *via* a metal–ene reaction: a mechanistic study†

Joshua P. Barham, *[a,b] Thierry N. J. Fouquet [a] and Yasuo Norikane [a]

Received 19th November 2019,
Accepted 26th January 2020

DOI: 10.1039/c9ob02495f

rsc.li/obc

Base-catalyzed, C-alkylation of potassium (K) enolates with styrenes (CAKES) has recently emerged as a highly practical and convenient method for elaboration or synthesis of pharmaceutically-relevant cores. K enolate-type precursors such as alkyl-substituted heterocycles (pyridines, pyrazines and thiophenes), ketones, imines, nitriles and amides undergo C-alkylation reactions with styrene in the presence of KO*t*Bu or KHMDS. Surprisingly, no studies have probed the reaction mechanism beyond the likely initial formation of a K enolate. Herein, a synergistic approach of computational (DFT), kinetic and deuterium labelling studies rationalizes various experimental observations and supports a metal–ene-type reaction for amide CAKES. Moreover, our approach explains experimental observations in other reported C-alkylation reactions of other enolate-type precursors, thus implicating a general mechanism for CAKES.

Introduction

The addition of simple pre-made alkyllithium compounds to styrenes is a known reaction[1] and is used in anionic polymerization chemistry.[2] While the addition of alkylpotassiums to styrenes is rare, in recent years, C-Alkylation of K Enolates with Styrenes (CAKES) is emerging as a practical, convenient, high-yielding method for elaboration or synthesis of pharmaceutically-relevant cores.[3–5] KO*t*Bu-catalyzed CAKES of alkyl-substituted heterocycles (pyridines, pyrazines, thiophenes) were reported around five decades ago (Fig. 1A)[6] and the scope of alkylpyridine CAKES was recently extended by Guan *et al.*, using KHMDS and elevated temperatures (*ca.* 100 °C).[4] KO*t*Bu-catalyzed ketone, imine and nitrile CAKES was reported two decades ago by Knochel *et al.* (Fig. 1B), but no mechanistic rationale was available at that time.[3] Pines first reported KO*t*Bu-catalyzed amide CAKES;[7] using *N*-methyl-2-pyrrolidinone (NMP) and *N*-methyl-2-piperidone (NMPI) as substrates. Historically, C-alkylation of most aforementioned substrates is accomplished *via* initial deprotonation employing a strong base (NaH, LDA, *sec*-BuLi).[8]

Such reactions require an inert atmosphere, moisture-free conditions and cryogenic temperatures. In contrast, KO*t*Bu-mediated amide CAKES are performed successfully at elevated temperatures (>80 °C), under air and ambient moisture if stoichiometric base is used (Fig. 1C),[5] and are applicable to a variety of amides beyond NMP and NMPI (including acyclic alkylamides). Kobayashi *et al.* recently reported successful amide CAKES at rt with catalytic quantities (5–6 mol%) of base (KHMDS) and 18-crown-6 as a promotor under inert (Ar) atmosphere.[9] The term 'CAKES' is coined due to the general requirement for potassium bases; sodium bases succeed under certain conditions but reactions are sluggish, requiring higher temperatures or complexing additives.[4,5]

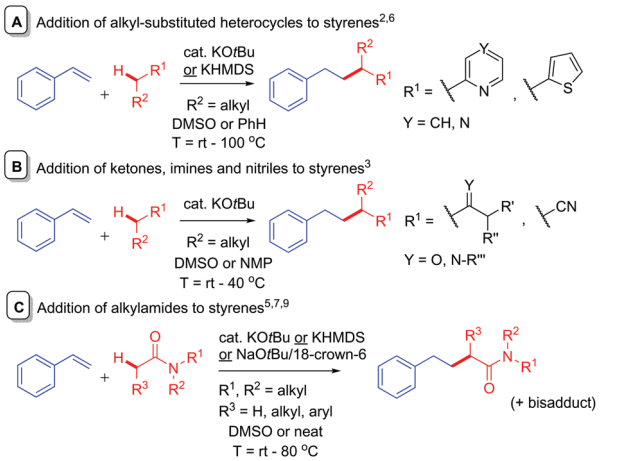

Fig. 1 Reported additions of potassium enolate-type precursors to styrenes.

[a]*National Institute of Advanced Industrial Science and Technology, Tsukuba Central 5, 1-1-1 Higashi, Tsukuba, Ibaraki 305-8565, Japan. E-mail: j.barham@saidagroup.jp*
[b]*SAIDA FDS INC., 143-10, Isshiki, Yaizu, Shizuoka, 425-0054, Japan*

†Electronic supplementary information (ESI) available: Experimental procedures, key NMR spectra, UV-visible absorption studies, EPR studies, kinetic plots, computational studies and coordinates. See DOI: 10.1039/C9OB02495F

Base-catalyzed CAKES reactions have been proposed to proceed *via* initial formation of a K enolate,[4–7,9] yet little evidence has actually been presented for this species.[10] This is especially curious given that the pK_a values of K enolate precursors like 4-methylpyridine,[11] acetonitrile[12] and *N*,*N*-dimethylacetamide[13] are considerably higher (pK_a = 31–35 in DMSO) than those of the conjugate acids of bases employed like HO*t*Bu[14] and HMDS (pK_a = 26–29 in DMSO).[14] Previous studies have then proposed the formal nucleophilic addition of the K enolate to styrene,[7,9] the direct outcome of which is a strongly basic benzylic alkylpotassium which appears to be considerably higher in energy than its K enolate and styrene precursors (the pK_a of PhMe is *ca.* 43 in DMSO).[15] Despite this, no evidence for a transition state (T.S.) or even rationale, to explain how such an endergonic process might occur, has been presented. The free energy barrier to such a T.S. would have to be low enough to be accessible at rt or the somewhat elevated temperatures often employed. Oligomers are not observed, suggesting the benzylic alkylpotassium is stabilized and cannot undergo addition to a second styrene. This implicates the heteroatom of the K enolate precursor (for example, the O atoms of alkylamides or N atoms of alkylpyridines) in coordinating a closed-type T.S. and in stabilizing the benzylic alkylpotassium as recently proposed by us (Fig. 2).

To our knowledge, computation has not yet been undertaken to probe the T.S. and energetics of CAKES reactions. Herein, we disclose a detailed mechanistic model constructed by a synergy of computational (DFT), kinetic and deuterium labelling studies, revealing a metal–ene T.S. in *N*-alkylamide CAKES. Various experimental observations are rationalized; such as the bisadduct/monoadduct (B/M) selectivity, the effect of styrene electronics, the roles of additives (18-crown-6) and bases (NaO*t*Bu *vs.* KO*t*Bu) in the reaction and the reactivity differences between acyclic *vs.* cyclic amide substrates. Moreover and importantly, our mechanistic picture accords with observations in other (ketone and alkylpyridine) CAKES, thus implicating our model as a general mechanism for each class of compound.

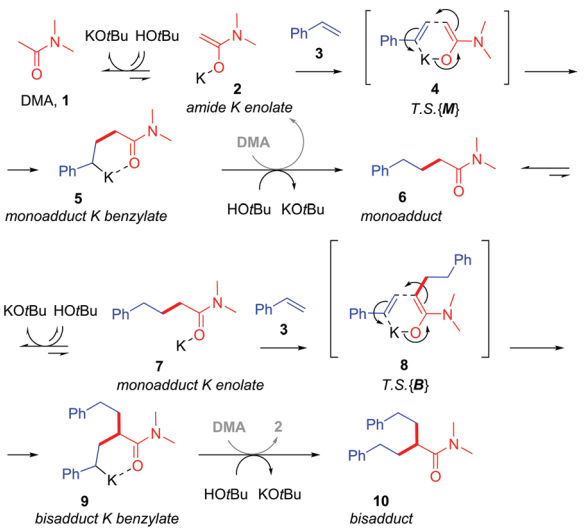

Fig. 2 Proposed metal–ene reaction mechanism.

Results and discussion

Investigation of bisadduct/monoadduct selectivity

In our recent study,[5] we found that the B/M selectivities of less-reactive acyclic amides such as *N*,*N*-dimethylacetamide (DMA, **1**) were heavily influenced by the styrene electronics (**3**, **11**–**17**). Monoadduct **6** is the expected main product because (i) a larger concentration of DMA (as solvent) than **6** occurs throughout the reaction and (ii) the rate of bisadduct **10** formation is limited by the concentration of **6** which is zero at T = 0 and increases during the reaction. Notwithstanding this, we reasoned the influence of styrene electronics on B/M selectivity could be rationalized by the free energy difference ($\Delta\Delta G_{rel}$) between the respective T.S. free energies leading to bisadduct ($\Delta G_{rel}\{\mathbf{B}\}$) and monoadduct products ($\Delta G_{rel}\{\mathbf{M}\}$) relative to their initial starting materials.[16] This was deemed a more robust method than comparing the difference in formal T.S. energy barriers relative to their respective K enolate precursors ($\Delta\Delta G^{\ddagger} = \Delta G^{\ddagger}\{\mathbf{B}\} - \Delta G^{\ddagger}\{\mathbf{M}\}$), because the second (monoadduct) deprotonation step is affected by the nature of the styrene and contributes to the overall bisadduct formation rate.

DFT calculations used the M06-2X functional[17] with a 6-31++G(d,p) basis set[18] on all atoms (except Br atoms, to which a pseudo-potential was applied).[19] The C-PCM implicit solvent model,[20] as implemented in Gaussian09,[21] assumed DMA, DMSO or PhH, depending on the reactions investigated. This was more appropriate than modelling explicit solvation in order to build a general model which could be applied to several different reaction classes. Results were compared to those from the B3LYP (unrestricted) functional[22] with a 6-31+G (d,p) basis set (see ESI†).[23] Fig. 3 shows the computed free energy profile of the proposed reaction mechanism (Fig. 2) for four styrenes in DMA (**1**) solvent. Fig. 4 shows the T.S. for deprotonation of **1** by KO*t*Bu (T.S.{**Deprot1**}) and the metal–ene T.S. **4** (T.S.{**M**}).

It was assumed that KO*t*Bu deprotonates **1** and is regenerated by deprotonation of HO*t*Bu by monoadduct K benzylate **5** to afford **6** (likewise for the pathway to **10**). Since benzylic alkylpotassium **5** (and **9**) are more potent bases than KO*t*Bu, it was proposed their deprotonation of **1** (or **6**) propagates a catalytic cycle.[5,9] Yet the stark pK_a difference between **1**/**6** and HO*t*Bu is likely more important than their available concentration difference and favors the reaction pathway regenerating KO*t*Bu. In support of this, computation found the T.S. for deprotonation of **1** by **5** ($\Delta G^{\ddagger}_{deprot}$ = 15.9 kcal mol^{-1}) was less accessible than that of deprotonation of **1** by KO*t*Bu ($\Delta G^{\ddagger}_{deprot}$ = 13.1 kcal mol^{-1}); deprotonation of HO*t*Bu was a much more kinetically accessible pathway for **5** ($\Delta G^{\ddagger}_{deprot}$ = 0.3 kcal mol^{-1}). Reactions of **1** with various styrenes were all exergonic with accessible free energy barriers ($\Delta G^{\ddagger 1}$ = 16.2–22.0 kcal mol^{-1}) at the previously applied[5] reaction temperatures (Table 1).[24]

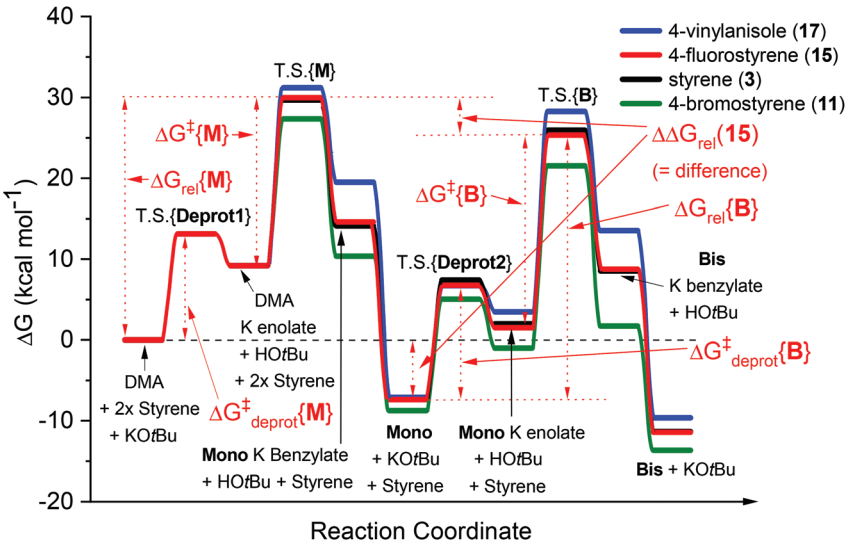

Fig. 3 Computed free energy profiles for reactions of DMA (**1**) with various styrenes in DMA solvent. The transition states for reactions of monoadduct K benzylate or bisadduct K benzylate with proton sources are not shown. DFT calculations were performed[17–22] with details as in ESI.†

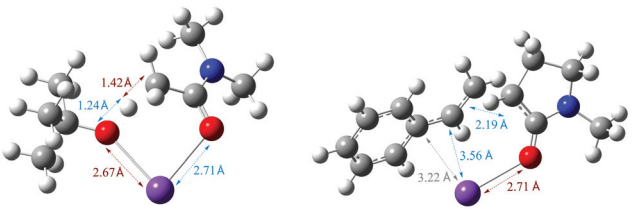

Fig. 4 Optimized structures for T.S.{**Deprot1**} and T.S.{**M**} for reaction of DMA, showing the lengths of forming and breaking bonds.

A larger $\Delta\Delta G_{rel}$ (= ΔG_{rel}{**B**} − ΔG_{rel}{**M**}) means slower relative kinetics of the reaction of monoadduct (**6**) to give bisadduct (**10**) would direct styrene consumption towards the reaction of **1** to form **6**, hence decreasing the B/M ratio. Conversely, a smaller $\Delta\Delta G_{rel}$ would encourage bisadduct (**10**) formation and would increase the B/M ratio. Gratifyingly, a strong negative correlation was found between (i) the free energy difference between the transition states for formation of bisadducts and monoadducts ($\Delta\Delta G_{rel}$) and (ii) the B/M selectivity determined experimentally (Fig. 5). The outlier to this trend (not plotted) was **13**, which gave a relatively large $\Delta\Delta G_{rel}$ for its high B/M selectivity.

To probe further, we computed the free energy difference in the barriers for deprotonation (formation of amide K enolate *vs.* monoadduct K enolate), $\Delta\Delta G^{\ddagger}_{deprot}$, which affects the overall rate by controlling the available concentrations of reacting K enolate. For the reaction of **13**, $\Delta\Delta G^{\ddagger}_{deprot}$ was notably lower

Table 1 Transition state relative free energies for monoadduct ΔG_{rel}{**M**} and bisadduct formation ΔG_{rel}{**B**} for the reaction of acyclic amides with different styrenes and experimental selectivity

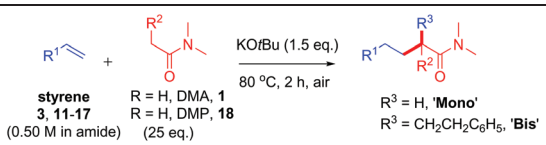

Entry	R^1/R^2	$\Delta G^{\ddagger 1}$ {**M**}	$\Delta G_{rel}{}^{a}$ {**A**}	$\Delta G_{rel}{}^{a}$ {**B**}	$\Delta\Delta G_{rel}$	$\Delta\Delta G^{\ddagger}_{deprot}$	B/M[b]
1	4-BrC_6H_5(**11**)/H	18.2	27.4	30.3	**2.9**	**0.6**	0.57
2	2-BrC_6H_5(**12**)/H	16.2	25.4	27.7	**2.3**	**0.3**	0.53
3	2-Py(**13**)/H	16.8	26.0	30.1	**4.1**	**0.1**	0.42
4	2-Naphthyl(**14**)/H	19.5	28.7	32.2	**3.6**	**1.5**	0.29
5	Ph(**3**)/H	20.5	29.7	33.3	**3.6**	**1.6**	0.29
6	4-FC_6H_5(**15**)/H	20.8	30.0	32.7	**2.7**	**1.0**	0.23
7	4-MeC_6H_5(**16**)/H	21.6	30.8	33.7	**2.9**	**1.0**	0.22
8	4-$MeOC_6H_5$(**17**)/H	22.0	31.2	35.4	**4.2**	**0.7**	0.06
9	Ph(**3**)/Me(**18**)	19.2	29.5	35.4	**5.9**	**5.1**	N/A

DFT calculations were performed[17–22] with details as in ESI.† For the computational profile of the DMP + styrene reaction, see ESI.† [a] Free energies (kcal mol^{-1}) relative to the initial starting materials (amide + 2*x* styrene + KO*t*Bu), see ESI† for further details. [b] Bis/mono selectivities were determined by the ^1H NMR yields of the crude reaction products in a previous report as previously described.[5]

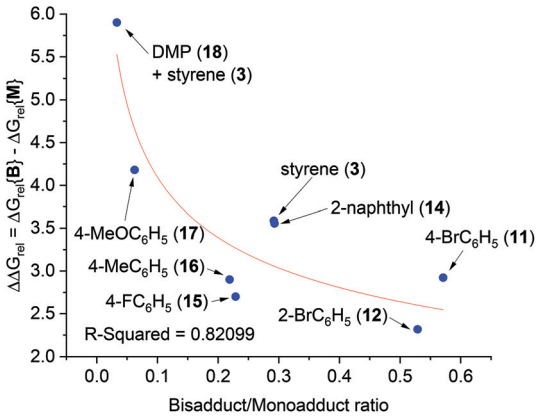

Fig. 5 Free energy difference ($\Delta\Delta G_{rel}$) between T.S.{**B**} and T.S.{**M**} *vs.* bisadduct/monoadduct ratio for reactions of DMA with various styrenes.

than other reactions, offsetting effect of $\Delta\Delta G_{rel}$. For **17**, a very high $\Delta\Delta G^{\ddagger}_{deprot}$ reinforced the large $\Delta\Delta G_{rel}$ in explaining a very low B/M selectivity. For *N*,*N*-dimethylpropionamide (DMP, **18**) + styrene, which gave exclusive monoadduct formation, $\Delta\Delta G^{\ddagger}_{deprot}$ was very high and was likely influential on the B/M selectivity. In fact, $\Delta G^{\ddagger}_{deprot}${**B**}, was approaching (85% the value of) the value of $\Delta G^{\ddagger}${**B**}. In all other cases, values of $\Delta G^{\ddagger}_{deprot}${**B**} varied between 56–74% of their respective $\Delta G^{\ddagger}${**B**}.

Investigation of styrene electronics and kinetics

We then proceeded to measure the kinetic profiles of reactions of DMA with the same selection of styrenes by *in situ* NMR spectroscopy using a variable temperature probe fixed at 80 °C (Table 2). As opposed to our previous study where reactions were prepared under ambient air/moisture,[5] herein kinetic study reactions were prepared within an N_2 glovebox in NMR tubes using commercial KO*t*Bu (sublimed grade 99.99%), DMSO-d_6 solvent (D, 99.9%) and degassed (3× freeze/pump/thaw) reagents (NMP/DMA/DMP) that had been dried overnight over activated 4 Å molecular sieves. Otherwise, KO*t*Bu/amide equivalents (relative to styrene) and order of addition accorded with the previous study.[5] Reactions were first order with respect to styrene, with Fig. 6 showing a non-linear positive relationship between the ratio of experimental (initial)[25] rate constants, (Ln(***k***)/Ln(***k*****$_0$**); ***k*** and ***k*****$_0$** refer to the reactions of styrene derivative and styrene, respectively) and the ratio of computed free energy barriers for the first metal–ene T.S. ($\Delta G''^{\ddagger}${**M**}/$\Delta G'^{\ddagger}${**M**}; superscripts ″ and ′ refer to the reactions of styrene derivative and styrene, respectively).

Here, the free energy barriers ($\Delta G^{\ddagger}$, not ΔG_{rel}) are examined on the logical assumption that the initial rates correspond to the formation of the monoadduct and are unaffected by formation of the bisadduct. Fig. 6 identifies the initial metal–ene reaction (T.S.{**M**}) as a rate-determining step (RDS) for styrene conversion, strengthening the computational mechanistic model. Although a catalytic loading of KO*t*Bu (20 mol%) failed to deliver products under previously-reported ambient air/moisture conditions,[5] we confirm catalytic activity under air- and moisture-free conditions herein,[26] consistent with previous reports.[6,9] In fact, the reaction rate is unchanged (Table 2, entry 7 *vs.* entry 4). DMP (**18**) gave a notably faster reaction rate than DMA (**1**), despite a similar T.S. free energy barrier difference (entry 9 *vs.* entry 4). The effect of styrene electronics on the rate of reaction was clearly depicted by a linear Hammett plot (Fig. 7),[27] demonstrating that all substrates proceed through the same T.S. and follow the same RDS. Notably, the configuration/bond distances of T.S.{**M**} (Fig. 4) for the reaction of DMA with styrene resemble those

Table 2 Rate constants for the conversion of various styrenes in the presence of DMA and DMP in DMSO-d_6 solvent

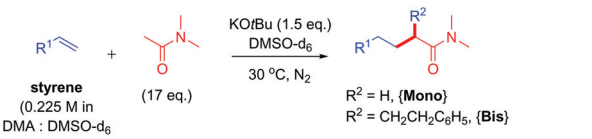

Entry	R^1	k ($\times 10^{-3}$)[a]	Ln(k) / Ln(k_0)	$\Delta G''^{\ddagger}${**M**}[b] / $\Delta G'^{\ddagger}${**M**}[c]
1	4-BrC_6H_5(**11**)[d]	22.730	0.482	0.886
2	4-FC_6H_5(**15**)	1.240	0.853	1.014
3	2-Naphthyl(**14**)	1.040	0.876	0.953
4	Ph(**3**)	0.392 (= k_0)	1.000	1.000 (= $\Delta G'^{\ddagger}$)
5	4-MeC_6H_5(**16**)[d]	0.135	1.136	1.055
6	4-$MeOC_6H_5$ (**17**)[d]	0.023	1.362	1.074
7[e]	Ph(**3**)	0.414	1.000	—
8[f]	Ph(**3**)	6.600	0.640[g]	0.937[h]

DFT calculations were performed[17–22] with details as in ESI.† [a] Experimentally-determined rate constant (s^{-1}) for conversion of styrene. [b] Free energy barrier relative to the amide K enolate precursor for the reaction of styrene derivative. [c] Free energy barrier relative to the amide K enolate precursor for the reaction of styrene. [d] Rate constant obtained from extrapolation of an Arrhenius plot due to impracticality of measuring the rate at 30 °C, see ESI† for details. [e] 25 mol% of KO*t*Bu was employed. [f] *N*,*N*-Dimethylpropionamide (DMP, **18**) was used instead of DMA. [g] Here, ***k*** refers to the reaction of DMP (**18**) with styrene measured in DMP solvent. [h] Here, $\Delta G''^{\ddagger}$ refers to the reaction of DMP (**18**) with styrene (DMA solvent was assumed) and $\Delta G'^{\ddagger}$ refers to the reaction of DMA (**1**) with styrene.

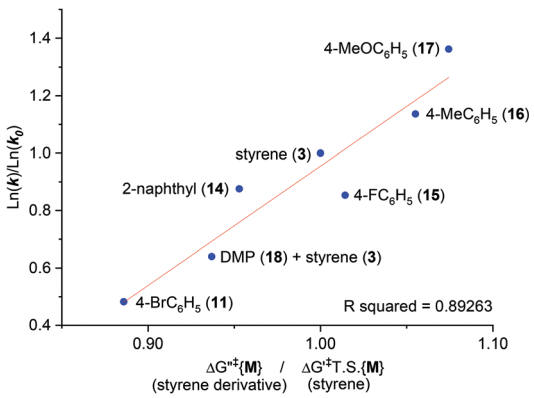

Fig. 6 Plot of the ratio of experimentally-determined rate constants relative to that of the styrene reaction *vs.* the ratio of free energy barriers for T.S.{Mono} relative to that of the styrene reaction.

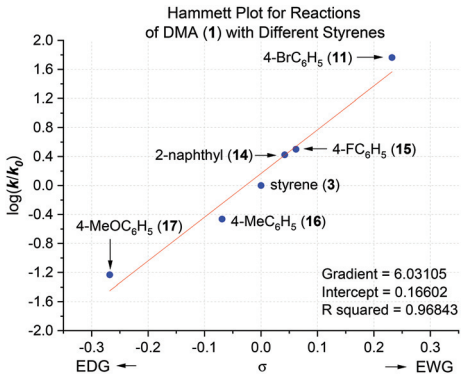

Fig. 7 Hammett plot for reactions of DMA with various styrenes.

previously reported for an analogous intramolecular reaction of an anionic oxime with a pendant styrene.[23e]

Investigation of cyclic amides

Next, we proceeded to examine the reactions of cyclic amides, such as NMP (**19**), with styrene as the 'electrophile' in DMSO solvent (Fig. 8). Compared to acyclic amides, cyclic amides like **19** give greater conversions over time and lower B/M selectivities (B/M = **20b**/**20a** = 0.13 for **19**).[5,28] Under similar[29] conditions, sarcosine anhydride (**21**) gave perfect monoadduct (**22a**) selectivity as previously reported.[5] Although the second reaction with styrene could take place at the alternative α-carbon to that of the first reaction, formation of **22a** and **22b** was assumed for fair computational comparison with **19**. The $\Delta\Delta G_{rel}$ (and $\Delta\Delta G_{deprot}$) value was more positive for reaction of **21** than reaction of **19**. Unfortunately, the reaction of sarcosine anhydride was not amenable to kinetic analysis by ^{1}H NMR under the standard conditions employed herein due to solubility issues. Next, we examined the previously-reported reactions of NMP with styrenes **3**, **15** and **17** (Fig. 9).[5]

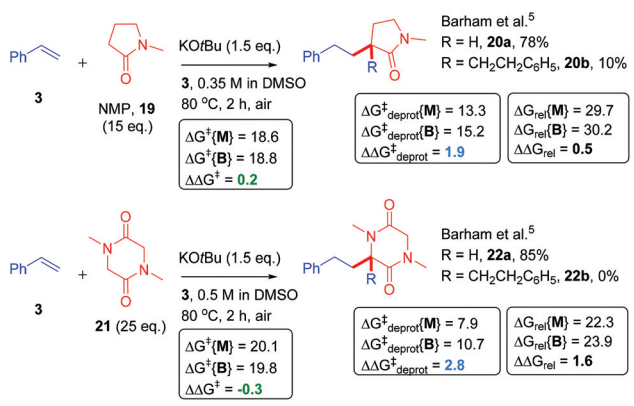

Fig. 8 Application of model to cyclic amide CAKES. Deprotonation and metal–ene-type T.S. barriers for monoadduct ($\Delta G^{\ddagger}_{deprot}${**M**} and $\Delta G^{\ddagger}${**M**}) and bisadduct formation ($\Delta G^{\ddagger}_{deprot}${**B**} and $\Delta G^{\ddagger}${**B**}) for the reaction of cyclic amides with styrene in DMSO solvent and their previously-reported experimental selectivity.[5] DFT calculations were performed[17–22] with details as in ESI.† Free energies are given in kcal mol^{-1}.

As opposed to DMA, the B/M selectivity of NMP's reactions with various styrenes was not influenced by styrene electronics. Computation (assuming DMSO solvent) resulted in a smaller difference in the range of $\Delta\Delta G_{rel}$ values (= 0.2 to 0.7) for all three styrene partners (Fig. 9), compared to that observed for DMA ($\Delta\Delta G_{rel}$ values = 2.3 to 4.2). Interestingly, $\Delta\Delta G^{\ddagger}_{deprot}$ values were very similar, allowing reassurance to directly compare the differences in free energy barriers for mono- *vs.* bisadduct formation ($\Delta\Delta G^{\ddagger}$), which were also similar. Kinetic profiles found the reaction of NMP faster than DMA, entirely consistent with a lower $\Delta G^{\ddagger}${**M**} for NMP (together with a slightly lower $\Delta G^{\ddagger}_{deprot}${**M**} and lower ΔG_{rel}{**M**}) as found by computation. The free energy barriers for monoadduct formation ($\Delta G^{\ddagger}${**M**}) were in the order **3** ≤ **15** ≪ **17** (Fig. 10), entirely consistent with the order of rate constants. The aforementioned relationship between Ln(***k***)/Ln(***k*$_0$**) and $\Delta G'^{\ddagger}${**M**}/$\Delta G^{\ddagger}${**M**} holds, confirming the overall rate of acyclic amides CAKES is determined by $\Delta G^{\ddagger}${**M**}. Counterintuitively, for **3**, **15** and **17**, the values of $\Delta\Delta G_{rel}$ are smaller for NMP than for DMA, yet NMP gives lower B/M selectivity. Here, $\Delta\Delta G^{\ddagger}_{deprot}$ (which determines the relative concentrations of available reacting amide K enolate and monoadduct K enolate) clearly

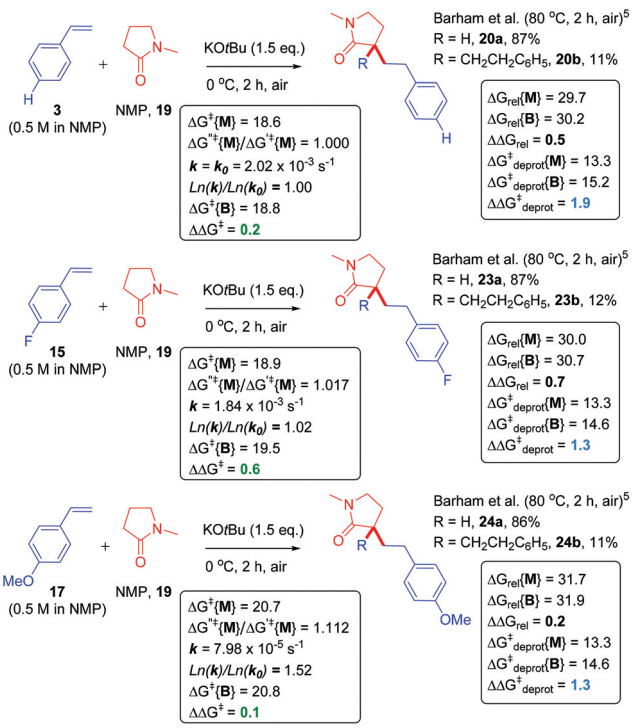

Fig. 9 Application of model to NMP CAKES with different styrenes. Deprotonation and metal–ene-type T.S. barriers and relative free energies (kcal mol^{-1}) for monoadduct ($\Delta G^{\ddagger}_{deprot}${**M**}, $\Delta G^{\ddagger}${**M**}, ΔG_{rel}{**M**}) and bisadduct formation ($\Delta G^{\ddagger}_{deprot}${**B**}, $\Delta G^{\ddagger}${**B**}, ΔG_{rel}{**B**}) for the reaction of NMP with various styrenes in DMSO solvent compared with their previously-reported experimental selectivity.[5] DFT calculations were performed[17–22] with details as in ESI.† Rate constant data was obtained in DMSO-d_6 solvent and under N_2 atmosphere, see ESI.† $\Delta G''^{\ddagger}$ and $\Delta G'^{\ddagger}$ refer to reactions of NMP (**19**) with styrene and styrene derivative, respectively.

becomes more influential than $\Delta\Delta G_{rel}$ as substitution increases at the K-enolate. For DMA + styrene (B/M = 0.292), $\Delta\Delta G^{\ddagger}_{deprot}$ = 1.6. For NMP + styrene (B/M = 0.128), $\Delta\Delta G^{\ddagger}_{deprot}$ = 1.9. For DMP + styrene (exclusive monoadduct), $\Delta\Delta G^{\ddagger}_{deprot}$ = 5.1.

Deuterium labelling investigation

Hartwig *et al.* highlighted the importance of conducting separate reactions in parallel to draw valid conclusions about KIEs.[30] Intramolecular[31] or intermolecular[32] competition experiments can present 'false positive' results that cannot conclusively identify the RDS (or turnover-limiting step).[33] Therefore, to further investigate the role of deprotonation in amide CAKES, NMP and NMP-d_9 were compared in parallel under conditions demonstrated affording incomplete conversion (10 min at 0 °C gave a 40% yield of **20a**) and were quenched after an identical time (Fig. 11A). Quantitative deuteration at the benzylic position confirmed the presence of a benzylic alkylpotassium. The decreased yield of **20a-d_9** highlighted the importance of deprotonation at the α-amido position, consistent with the observation of **20a-d_8** which likely formed *via* deprotonation of **20a-d_9**.[34] We then compared reactions of NMP and NMP-d_9 in parallel under slightly modified conditions using DMSO-d_6 solvent,[35] which allowed the reaction progress to be monitored over time by ^{1}H NMR spectroscopy. The initial rates of styrene conversion (k_H and k_D) were used to determine the KIE (KIE = 2.2).[25] This moderate primary KIE identifies one of two possibilities: (1) deprotonation is irreversible and is the RDS or (2) deprotonation is reversible and occurs before the RDS, such that an observed KIE results from an equilibrium isotope effect on that deprotonation step. The latter situation is likely considering the aforementioned (i) pK_a difference between HO*t*Bu and amides and (ii) influence of styrene electronics on the reaction rate.

After completion of the reactions by ^{1}H NMR (28 min for NMP + styrene *vs.* 51 min for NMP-d_9 + styrene), the yields and B/M selectivities for each reaction were similar. Although the reaction of NMP-d_9 + styrene in DMSO-d_6 was essentially complete after 51 min at 0 °C (see ESI†), it was left for extended time at rt prior to quenching. After quenching, workup and purification, the product ultimately isolated from the reaction was **20a-d_{10}** (which contained low abundances of **20a-d_9** and **20a-d_7** by mass spectrometry, see ESI†). The deuteration of benzylic positions in the presence of KO*t*Bu and deuterium sources (NMP-d_9 or DO*t*Bu) is feasible.[37]

Investigation of base, 18-crown-6, ambient air/moisture conditions and DMSO co-solvent

The moderate primary KIE observed is entirely consistent with the fact that C-alkylation reactions of amides with styrenes are dependent on the strength of base employed, with strong sodium/potassium bases such as KHMDS, NaHMDS, KO*t*Bu, KO*t*Am and KOH all giving successful reactions, while weak potassium bases KF, K_2CO_3 and weak organic bases DABCO and DBU gave no reaction under the same conditions.[5] Under the previously reported conditions (ambient air/moisture), NaO*t*Bu alone led to successful reaction of NMP but 18-crown-6 was required for successful reaction of DMA at 80 °C.[5] In addition, 18-crown-6 appeared to increase reactivity of DMA and NMP in the presence of KO*t*Bu (and NaO*t*Bu).[5] These observations are consistent with other reports of C-alkylation of weakly-acidic compounds with styrene[4,9] showing the rate-enhancing effects of 18-crown-6.

We elected to measure the kinetic profiles of reactions of NMP + styrene under different conditions (nature and equivalents of base, 18-crown-6 as an additive, use of ambient air/moisture) by *in situ* NMR spectroscopy (Table 3). Under the standard (air-and moisture-free) conditions herein, the reac-

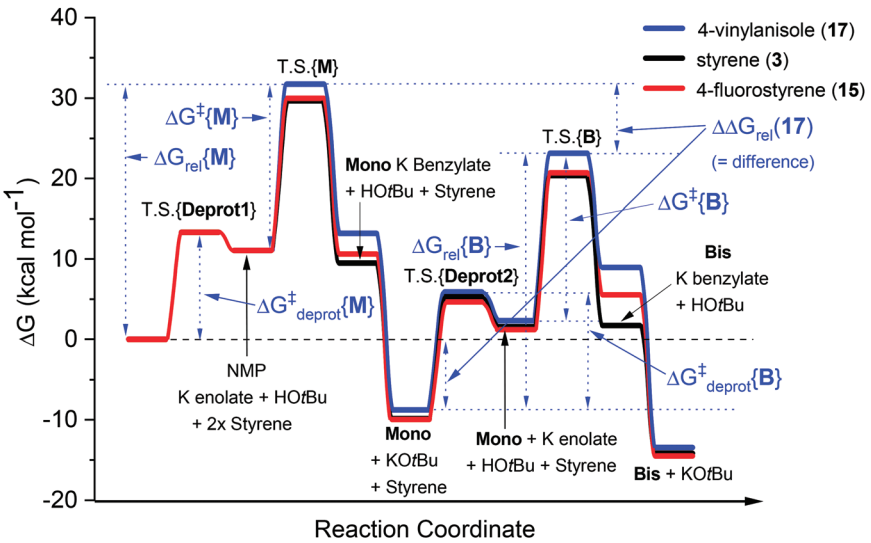

Fig. 10 Computed free energy profiles for reactions of NMP (**19**) with various styrenes. The transition states for reactions of monoadduct K benzylate or bisadduct K benzylate with proton sources are not shown. DFT calculations were performed[17–22] with details as in ESI.†

Table 3 Rate constants for the conversion of styrene in the presence of NMP and in DMSO-d_6 solvent

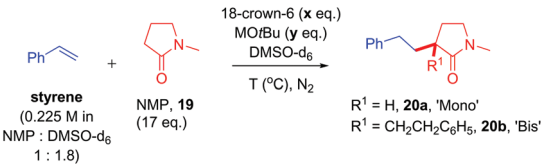

Entry	Conditions	k ($\times 10^{-3}$)[a]	$\Delta G^{\ddagger}_{\text{deprot}}$ [b]	ΔG_{rel} {Enolate}[b]
1	M = K, T = 0, x = 0, y = 1.5	2.020	13.3	11.1
2	M = K, T = 30, x = 0, y = 1.5	104.976[c]	—	—
3	M = K, T = 0, x = 0, y = 0.25	1.190	—	—
4[d]	M = K, T = 25, x = 0, y = 1.5	2.303	—	—
5[e]	M = K, T = 0, x = 1.5, y = 1.5	N/A[f]	−18.3	−6.3
6	M = Na, T = 80, x = 0, y = 1.5	2.750	21.3	12.7
7[e]	M = Na, T = 80, x = 1.5, y = 1.5	—	18.3	−4.5

DFT calculations were performed[17–22] with details as in ESI.† [a] Experimentally-determined rate constant (s^{-1}) for conversion of styrene. [b] Free energy ΔG_{rel} or free energy barrier $\Delta G^{\ddagger}_{\text{deprot}}$ relative to the initial starting materials for the deprotonation of styrene (*e.g.* amide + 2*x* styrene + KO*t*Bu for entry 1), see ESI† for further details. [c] Rate constant determined by extrapolating an Arrhenius plot (see ESI† for details). [d] The reaction was prepared under ambient air/moisture with non-degassed and non-dried fresh reagents. [e] For purposes of computation, the 18-crown-6/M^+ complex as an innocent bystander and formation of the "naked" amide enolate from *tert*-butoxide anion and NMP were assumed (see ESI†). [f] Styrene was fully converted at 0 °C before the first NMR scan (2 min); lower temperatures could not be employed due to reaction mixture freezing. Free energies given in kcal mol^{-1}.

tion of NMP proceeded rapidly at 0 °C (entry 1). Use of catalytic (25 mol%) KO*t*Bu *ca.* halved the reaction rate (entry 3) and gave **20a**,[38] in stark contrast to reactions of DMA where the same reaction rate was observed for either 25 mol% of 1.5 eq. KO*t*Bu. The reaction was significantly retarded by preparing under ambient air/moisture with non-degassed and non-dried solvents (as supplied), such that 25 °C was required to observe a similar rate constant to the reaction under standard conditions at 0 °C (entry 4 *vs.* entry 1). In line with the observed KIE, these observations confirm the deprotonation steps in the reaction mechanism (*e.g.* Fig. 12, pathway **A**) do influence the overall kinetics of amide CAKES. While styrenes are known as common radical acceptors at the terminal position,[39] amide CAKES proceeded successfully in air and in the presence of TEMPO (1 eq.) as reported previously,[5] and no radical species were detected by EPR spectroscopy studies herein (see ESI†).

The reaction rate was too fast to measure in the presence of 18-crown-6 (entry 5 *vs.* entry 1), confirming that 18-crown-6 promotes the reaction. Presumably, sequestering of potassium cation enhances the basicity of the *tert*-butoxide anion as is previously reported,[40] giving rise to a lower barrier for the transition state of deprotonation (Fig. 12, pathway **B** *vs.* **A**). Computationally, this was found to be the case (entry 5 *vs.* entry 1); $\Delta G^{\ddagger}_{\text{deprot}}$ was negative (barrierless) and the combined relative energy of products (ΔG_{rel}{**Enolate**}) was markedly lower for pathway **B**, even exothermic. Substitution of KO*t*Bu with NaO*t*Bu significantly retarded the reaction; the use of NaO*t*Bu required 80 °C to observe a comparable rate constant (Table 3, entry 6 *vs.* entry 1) consistent with a higher $\Delta G^{\ddagger}_{\text{deprot}}$. Promotion of the NaO*t*Bu-mediated reaction by 18-crown-6 as disclosed previously[5] is rationalized by the reaction of the "naked" *tert*-butoxide anion with NMP and an 18-crown-6/Na^+ complex having a lower $\Delta G^{\ddagger}_{\text{deprot}}$ (entry 7 *vs.* entry 6). That an exotherm was observed when KO*t*Bu and 18-crown-6 were mixed in NMP (before styrene addition), but not in the case of NaO*t*Bu, is consistent with ΔG_{rel} values in pathway **B**. Alternative scenarios, like deprotonation of an 18-crown-6/M cation/NMP complex by "naked" *tert*-butoxide anion, or deprotonation of NMP by an 18-crown-6/MO*t*Bu complex, were investigated computationally (see ESI†). Although such scenarios cannot be ruled out, the former could not account for the experimentally observed exotherm while the latter gave a T.S. too hindered to be computed.

Rate enhancement in a mechanistic step following the initial deprotonation cannot be ruled out at this stage. While computation of a metal–ene-type T.S. involving co-ordination of 18-crown-6 was too sterically encumbered and led to dissociation, the reversibility of K^+/Na^+ complexation by 18-crown-6 increases markedly in DMSO/amide-based solvents[41] such that solvated K^+/Na^+ may still be available to construct the metal–ene-type T.S. A non-cyclic, open T.S. in which potassium cation is absent cannot be ruled out (see ESI† and later discussion on 4-alkylpyridine). Nonetheless, a strong argument can be made for rate acceleration *via* pathway **B** due to the observed KIE. It is possible that other rate-enhancing additives (LiCl/PMDTA)[31,42] used in these types of reactions function *via* a similar mechanism.

DMSO has been employed as a co-solvent in previous reports of C-alkylations with styrene, allowing the K-enolate precursor substrate loading to be lowered.[3,5,7] For the purposes of kinetic NMR studies herein, DMSO-d_6 was employed as a co-solvent. Therefore, we desired to probe the role of DMSO-d_6. When reactions in DMSO-d_6 co-solvent were compared to reactions using the amide substrate (DMA or NMP) as solvent (quenched after a given time), we found higher product yields in the former case.[26,38] Elsewhere, it is known that solvation of

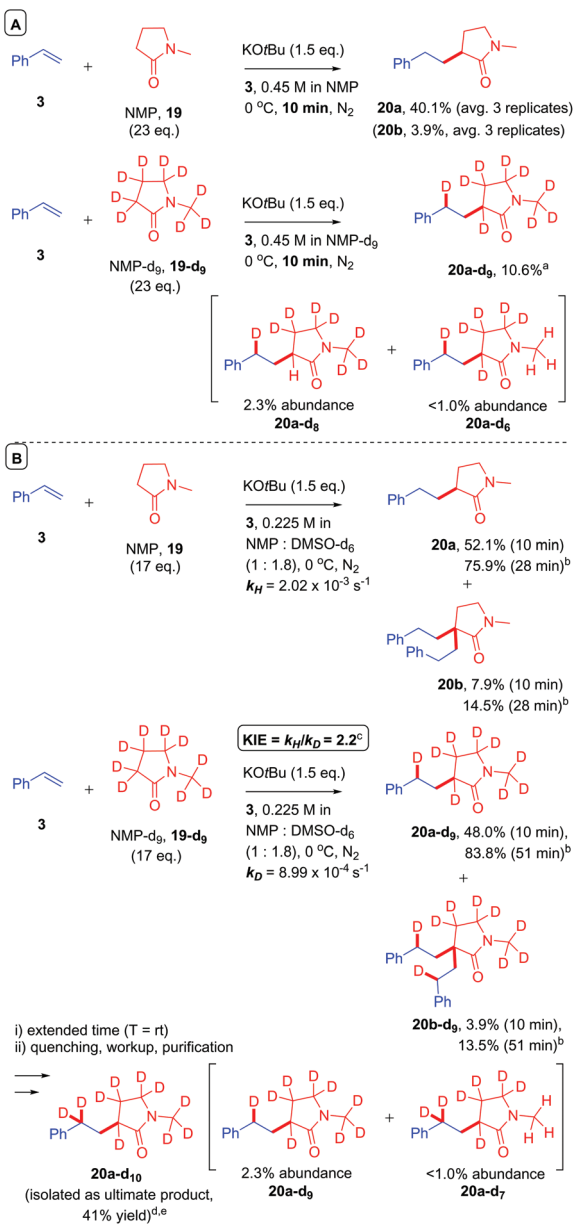

Fig. 11 Deuterium labelling experiments. Unless otherwise stated, yields were determined by ^{1}H NMR by comparison to 1,3,5-trimethoxybenzene (1.0 eq.) as an internal standard. Structures of deuterated products were established by MALDI and ESI-MS (see ESI†). [a] Abundances of partially-deuterated compounds **20a-d$_8$** and **20a-d$_6$** were determined relative to the ionization of **20a-d$_9$** at 100%.[36] [b] Reaction was deemed complete (<5% styrene) at this time. [c] KIE was determined based on the conversion of styrene over time and by comparison to 1,3,5-trimethoxybenzene (1.0 eq.) as an internal standard (see ESI†). [d] Following 1 h of reaction time at 0 °C the reaction was allowed to warm to rt and product **20a-d$_{10}$** isolated after extended time (see ESI†). [e] Abundances of partially-deuterated compounds **20a-d$_9$** and **20a-d$_7$** were determined relative to the ionization of **20a-d$_{10}$** at 100%.[36]

KO*t*Bu in DMSO increases the basicity of the *tert*-butoxide anion.[43] Deuterated products were not observed in any reactions of non-deuterated DMA or NMP using DMSO-d$_6$ as solvent. Given the similar B/M selectivity with *vs.* without DMSO solvent (Fig. 11) and previous literature results that have used DMSO/NMP interchangeably,[3,5,7] there is no reason to suspect a role for DMSO/dimsyl anion[44] in the reaction mechanism beyond promoting base reactivity or stabilizing intermediates/T.S.es.

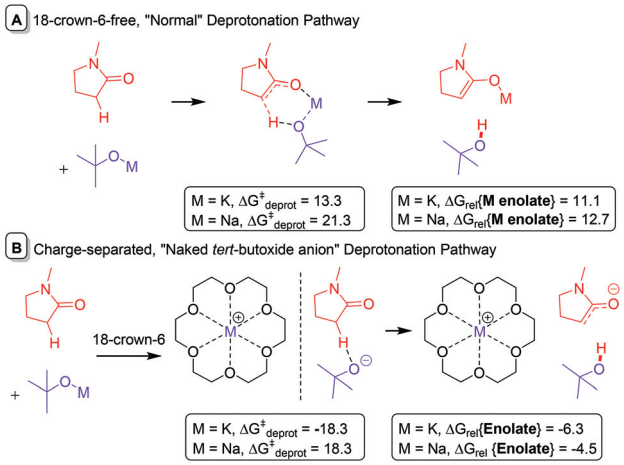

Fig. 12 Pathways for deprotonation of NMP by KO*t*Bu/NaO*t*Bu in absence and presence of 18-crown-6. Free energies are given in kcal mol^{-1}. DFT calculations were performed[17–22] with details as in ESI.†

A general mechanism for C-alkylation with styrenes

Based on the fact that monoadduct and bisadduct products have been observed in other previously reported C-alkylation reactions,[3,4] we postulated that the previously-mentioned metal–ene-type mechanism may be a general pathway for this recently trending class of reaction and applied our computational model accordingly. The C-alkylation of cyclohexanone (**25**) with styrene reported by Knochel gave good selectivity for the monoadduct **26a** (60% yield) and some bisadduct **26b** (B/M = 0.15),[45] whereas the reaction of α-tetralone (**27**) gave monoadduct **28a** (68% yield) and no bisadduct (**28b**) was reported. In order to confirm whether the bisadduct **28b** was formed or not, the reaction of **27** was repeated. In our hands, the reaction gave **28a** (85% yield) and **28b** (11% yield) as determined by NMR analysis of the crude reaction products by comparison to an internal standard. Thus, a marginally higher selectivity for monoadduct **28a** was observed in the reaction of α-tetralone (B/M = 0.13).[46] The reactions were then computed according to our model which successfully found metal–ene T.S.es for each reaction. In line with the B/M selectivity difference, α-tetralone gave both a more positive $\Delta\Delta G_{rel}$ than **25** and a more positive $\Delta\Delta G^{\ddagger}_{deprot}$ (Fig. 13). The free energy barriers for the first metal–ene T.S. ($\Delta G^{\ddagger}${**M**}) were almost identical for **25** and **27**. That $\Delta G^{\ddagger}_{deprot}${**M**} was more positive for **27** contrasted with the faster kinetics of **27**, revealing a limitation in the current model which could not account for the known acidifying effect of the arene on the α-carbon of the ketone.[47] Overall,

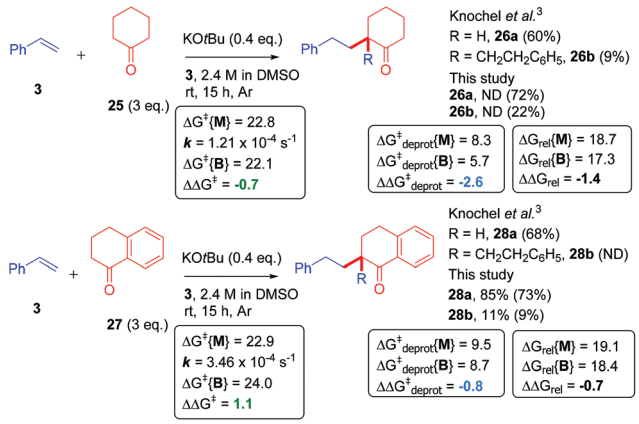

Fig. 13 Application of model to ketone CAKES. ND, not determined. Transition state relative free energies (kcal mol^{-1}) for monoadduct (ΔG_{rel}{M}) and bisadduct formation (ΔG_{rel}{B}) for the reaction of cyclic ketones with styrene in DMSO are compared with their previously-reported experimental selectivity.[3] DFT calculations were performed[17–22] with details as in ESI.† Rate constant data was obtained using DMSO-d_6 as solvent, see ESI.† Yields were determined by ^{1}H NMR by comparison to 1,3,5-trimethoxybenzene (1.0 eq.) as an internal standard. Isolated yields are shown in parenthesis.

ketone CAKES seem to follow a similar mechanism to amide CAKES.

Finally, the reactions of alkylpyridines with styrene in benzene, as reported by Guan,[4] were investigated. Here, the previously-reported[4] B/M selectivity shifted drastically when comparing 2-methylpyridine (**29**) (B/M = 0.28) to 4-methylpyridine (**31**) (B/M = 1.38). This led Guan to propose an interaction between the pyridyl N atom and the catalyst (KHMDS) facilitated the catalytic C–H alkylation reaction. Herein, computation showed that the potassium cation interacted strongly with the pyridyl N atom as well as the π-system of styrene in the T.S. of the 2-methylpyridine (**29**) reaction. The consequence of this interaction was a more hindered T.S. in the case of the bisadduct formation. As expected, the $\Delta\Delta G_{rel}$ for 2-methylpyridine reaction was more positive than that of the 4-methylpyridine reaction and accorded with the change in B/M selectivity (Fig. 14). This was reinforced by a more positive $\Delta\Delta G^{\ddagger}_{deprot}$ in the 2-methylpyridine reaction.

A substituted, cyclic 2-alkylpyridine (**33**) gave perfect monoadduct selectivity,[4] in accordance with decreased B/M selectivity observed for cyclic/substituted *vs.* acyclic/unsubstituted amides (such as DMA *vs.* NMP observed earlier) and in accordance with both its more positive $\Delta\Delta G_{rel}$ and more positive $\Delta\Delta G^{\ddagger}_{deprot}$ than **29**. The reaction of 2-methylquinoline (**35**), which gave slightly lower B/M selectivity *vs.* **29**,[4] had a marginally more positive $\Delta\Delta G_{rel}$ value (despite a less positive $\Delta\Delta G^{\ddagger}_{deprot}$ value). The reaction of monoadduct **30a** gave exclusively **30b** when compared to the reaction of **29**, while the B/M selectivity in the reaction of monoadduct **32a** decreased (but was not exclusive for **32b**) compared to the reaction of **31**.[4] The latter case could be explained by its more positive $\Delta\Delta G_{rel}$ and $\Delta\Delta G^{\ddagger}_{deprot}$ values compared to **31**, while the

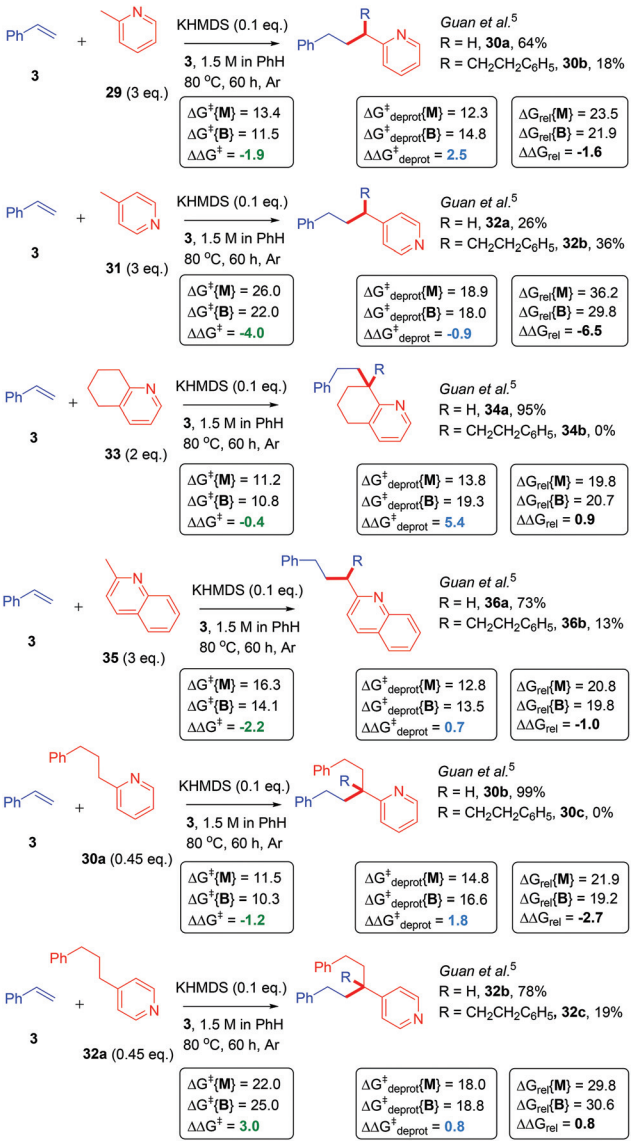

Fig. 14 Application of model to alkylpyridine CAKES. Transition state relative free energies for monoadduct (ΔG_{rel}{Mono}) and bisadduct formation (ΔG_{rel}{Bis}) for the reaction of alkylpyridines with styrene in PhH are compared with their previously-reported experimental selectivity.[4] DFT calculations were performed[17–22] with details as in ESI.† For reactions of **30a** and **32a**, yields previously reported are based on the alkylpyridine starting material.[4] ND, not determined.

former case showed a discrepancy between the computation and B/M selectivity, revealing a limitation in the model. Overall, results are consistent with previous observations for amide CAKES (DMA *vs.* DMP *vs.* NMP), suggesting that $\Delta\Delta G_{rel}$ tends to govern B/M selectivity for alkylpyridine CAKES where the K-enolate motif is unsubstituted, while $\Delta\Delta G^{\ddagger}_{deprot}$ tends to govern B/M selectivity where the K-enolate motif is substituted/cyclic.

It is noted that the metal–ene-type T.S. proposed herein is geometrically inaccessible for the reaction of 4-alkylpyridine. This reaction must proceed *via* an open T.S. where the potass-

ium cation is absent (is bound to the pyridine lone pair instead), hence the T.S. suffers a significantly higher free energy barrier $\Delta G^{\ddagger}$. This can be seen when comparing $\Delta G^{\ddagger}$ or ΔG_{rel} values in the reactions of **29** *vs.* **31**, or **30a** *vs.* **32a**. While the heteroatom-stabilized metal–ene-type T.S. is favored, the open T.S. is accessible at high enough temperatures/with strong enough base.[48] A moderate primary KIE (2.7–3.3) was observed by Guan for this KHMDS-catalyzed reaction of alkylpyridines with styrene and it was concluded that the C–H cleavage step was the RDS.[4] However, since the reactivity therein similarly was influenced by the electronics of the styrene (this was also reported by Knochel[3]) and since the moderate primary KIE is similar to that observed herein, it is postulated that the mechanistic picture for alkylpyridine CAKES reflects the scenario of NMP (**19**) herein: a reversible C–H cleavage step which influences the concentration of reacting alkylpotassium species and is subject to a KIE, followed by a higher energy, rate-determining metal–ene-type transition state.

Based on the results of this study, we propose a general working mechanism for CAKES (Fig. 15). Deprotonation of the enolate precursor by the potassium base proceeds *via* an equilibrium to generate a low concentration of K enolate. Although K enolates could not be observed previously[4] or herein by ^{1}H NMR, we tentatively propose their detection by UV-vis spectroscopy analysis of the colored reaction mixture (see ESI†). This deprotonation step is a minor contributor to the overall rate by controlling the available equilibrium concentration of K enolate and it can be influenced by the choice and loading of base as well as co-ordinating additives. The K enolate then undergoes addition to the styrene *via* a metal–ene reaction, which is the RDS (major contributor to the overall rate) and the turnover-limiting step. Deprotonation of the *in situ*-formed conjugate acid by the K benzylate is kinetically favoured, completing the CAKES catalytic cycle. The metal–ene-type reaction involving K enolates is in accordance with expectations from intramolecular magnesium–ene reactions of Grignard reagents (or those of alkyllithium or alkylzinc reagents)[49] first reported by Lehmkuhl[50] and popularized by Oppolzer[51] in the 1980s. To our knowledge, this study confirms the first example of a metal–ene-type reaction involving K enolates.

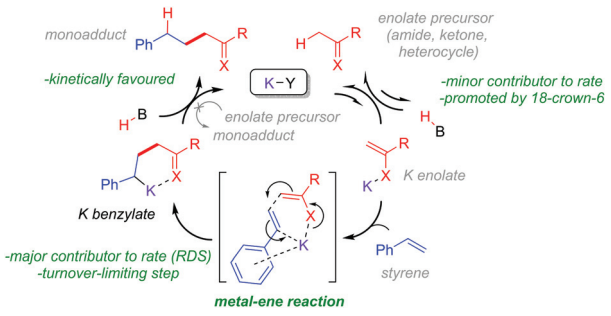

Fig. 15 Proposed general metal–ene reaction mechanism.

Conclusions

Base-catalyzed amide CAKES have been studied using a synergistic approach of computation and experimental kinetic studies. A mechanism proceeding through metal–ene-type transition states sufficiently explains experimental selectivity and reactivity (rate) differences when different styrene partners or different amide partners are used. The role of additives 18-crown-6 is rationalized. Computational barriers are accessible at the reaction temperatures employed and agree with rate constants obtained by kinetic data, thus corroborating a pathway proceeding through a benzylic alkylpotassium species. Notably, our mechanistic picture explains the experimental observations in other (ketone and alkylpyridine) CAKES, hence gathering all these reaction classes under the umbrella of a general reaction mechanism. We hope that this study might shed light on related reactivity[31,52] in this field. Further investigations are ongoing in our laboratory.

Conflicts of interest

There are no conflicts to declare.

Acknowledgements

We thank Dr Kazuhiko Yamasaki (AIST, Tsukuba) for assistance and advice on NMR. We thank Mrs Sayaka Nakamura and Prof. Hiroaki Sato (AIST, Tsukuba) for assistance with MALDI-HRMS, ESI MS and MS MS analysis. We thank Dr Yoong-Kee Choe (AIST, Tsukuba) for advice on DFT calculation methods. We thank Mr Masato Yamazoe and Prof. Kazuhiro Morimoto (University of Tsukuba) and Prof. John C. Walton (University of St. Andrews) for assistance with EPR measurements and interpretation of spectra, respectively. We thank Dr Daniel T. Payne (NIMS, Tsukuba) for helpful discussions. J. P. B. is a former JSPS International Research Fellow and is grateful for financial support from JSPS. This work was supported by JSPS KAKENHI Grant Number JP18F19030.

Notes and references

1 For examples, see: (*a*) T. Fujita, S. Watanabe, K. Suga and H. Nakayama, *Synthesis*, 1979, 310–311; (*b*) H. Pines and N. E. Sartoris, *J. Org. Chem.*, 1969, **34**, 2113–2118; (*c*) X. Wei and R. J. K. Taylor, *Chem. Commun.*, 1996, 187–188.

2 For examples, see: (*a*) M. Merton, *Anionic Polymerisation: Principles and Practice*, Academic Press, New York, 1983, pp. 13–85; (*b*) R. Waack and M. A. Doran, *J. Org. Chem.*, 1967, **32**, 3395–3399.

3 (*a*) A. L. Rodriguez, T. Bunlaksunanusom and P. Knochel, *Org. Lett.*, 2000, **2**, 3285–3287; (*b*) T. Bunlaksunanusom, A. L. Rodriguez and P. Knochel, *Chem. Commun.*, 2001, 745–746.

4 D. Zhai, X. Zhang, Y. Liu, L. Zheng and B.-T. Guan, *Angew. Chem., Int. Ed.*, 2018, **57**, 1650–1653.
5 J. P. Barham, S. Tamaoki, H. Egami, N. Ohneda, T. Okamoto, H. Odajima and Y. Hamashima, *Org. Biomol. Chem.*, 2018, **16**, 7568–7573.
6 H. Pines and W. M. Stalick, *Tetrahedron Lett.*, 1968, **34**, 3723–3726. For an addition to styrene in the presence of dispersed potassium or sodium, see: H. Pines and N. E. Sartoris, *J. Org. Chem.*, 1969, **34**, 2113–2118.
7 Styrenes as well as trimethylvinylsilane, butadiene and isoprene can be employed in the case of cyclic alkylamides, see: H. Pines, S. V. Kannan and J. Simonik, *J. Org. Chem.*, 1971, **36**, 2311–2315.
8 For selected examples, see: (*a*) W. S. Fones, *J. Org. Chem.*, 1949, **14**, 1099–1102; (*b*) R. P. Woodbury and M. W. Rathke, *J. Org. Chem.*, 1978, **43**, 881–884; (*c*) P. Beak and W. J. Zajdel, *J. Am. Chem. Soc.*, 1984, **106**, 1010–1018; (*d*) P. Beak and W. K. Lee, *J. Org. Chem.*, 1990, **55**, 2578–2580; (*e*) R. K. Dieter, G. Oba, K. R. Chandupatla, C. M. Topping, K. Lu and R. T. Watson, *J. Org. Chem.*, 2004, **69**, 3076–3086; (*f*) R. B. Lettan II, C. V. Galliford, C. C. Woodward and K. A. Scheidt, *J. Am. Chem. Soc.*, 2009, **131**, 8805–8814.
9 Styrenes as well as heteroatom(P, Si and S)-substituted alkenes can be employed in the case of acyclic alkylamides, see: Y. Yamashita, R. Igarashi, H. Suzuki and S. Kobayashi, *Org. Biomol. Chem.*, 2018, **16**, 5969–5972.
10 In ref. 4, kinetic isotope effect (KIE) studies were used to infer that the rate determining step of the reaction of 2-methylpyridine with styrene was the initial benzylic C–H deprotonation. The proposed potassium enolate intermediate (potassium picoline) could not be observed when treating 2-methylpyridine with KHMDS only.
11 F. G. Bordwell, *Acc. Chem. Res.*, 1988, **21**, 456–463.
12 F. G. Bordwell, M. Van der Puy and N. R. Vanier, *J. Org. Chem.*, 1976, **41**, 1883–1885.
13 V. S. Bryantsev, J. Uddin, V. Giordani, W. Walker, D. Addison and G. V. Chase, *J. Electrochem. Soc.*, 2013, **160**, A160–A171.
14 S. Tabassum, O. Sereda, P. V. G. Reddy and R. Wilhelm, *Org. Biomol. Chem.*, 2009, **7**, 4009–4016.
15 F. G. Bordwell, D. Algrim and N. R. Varnier, *J. Org. Chem.*, 1977, **42**, 1817–1819.
16 For a recent example of similar computational rationalization of the experimental selectivity, see: J. P. Barham, M. P. John and J. A. Murphy, *J. Am. Chem. Soc.*, 2016, **138**, 15482–15487.
17 (*a*) Y. Zhao and D. G. Truhlar, *Acc. Chem. Res.*, 2008, **41**, 157–167; (*b*) Y. Zhao and D. G. Truhlar, *J. Chem. Phys.*, 2006, **125**, 194101.
18 (*a*) R. Krishnan, J. S. Binkley, R. Seeger and J. A. Pople, *J. Chem. Phys.*, 1980, **72**, 650–654; (*b*) M. J. Frisch, J. A. People and J. S. Binkley, *J. Chem. Phys.*, 1984, **80**, 3265–3269; (*c*) A. D. McLean and G. S. Chandler, *J. Chem. Phys.*, 1980, **72**, 5639–5648; (*d*) J.-P. Blaudeau, M. P. McGrath, L. A. Curtiss and L. Radom, *J. Chem. Phys.*, 1997, **107**, 5016–5021; (*e*) T. Clark, J. Chandrasekhar, G. W. Spitznagel and P. V. R. Schleyer, *J. Comput. Chem.*, 1983, **4**, 294–301.
19 A. Bergner, M. Dolg, W. Küchle, H. Stoll and H. Preuß, *Mol. Phys.*, 1993, **80**, 1431–1441.
20 (*a*) V. Barone and M. Cossi, *J. Phys. Chem. A*, 1998, **102**, 1995–2001; (*b*) M. Cossi, N. Rega, G. Scalmani and V. Barone, *J. Comput. Chem.*, 2003, **24**, 669–681.
21 (*a*) P. Hohenberg and W. Kohn, *Phys. Rev.*, 1964, **136**, B864–B871; (*b*) W. Kohn and L. Sham, *J. Phys. Rev.*, 1965, **140**, A1133–A1138; (*c*) M. J. Frisch, G. W. Trucks, H. B. Schlegel, G. E. Scuseria, M. A. Robb, J. R. Cheeseman, G. Scalmani, V. Barone, B. Mennucci, G. A. Petersson, H. Nakatsuji, M. Caricato, X. Li, H. P. Hratchian, A. F. Izmaylov, J. Bloino, G. Zheng, J. L. Sonnenberg, M. Hada, M. Ehara, K. Toyota, R. Fukada, J. Hasegawa, M. Ishida, T. Nakajima, Y. Honda, O. Kitao, H. Nakai, T. Vreven, J. A. Montgomery Jr., J. E. Peralta, F. Ogliaro, M. J. Bearpark, J. Heyd, E. N. Brothers, K. N. Kudin, V. N. Staroverov, R. Kobayashi, J. Normand, K. Raghavachari, A. P. Rendell, J. C. Burant, S. S. Iyengar, J. Tomasi, M. Cossi, N. Rega, N. J. Millam, M. Klene, J. E. Knox, J. B. Cross, V. Bakken, C. Adamo, J. Jaramillo, R. Gomperts, R. E. Stratmann, O. Yazyev, A. J. Austin, R. Cammi, C. Pomelli, J. W. Ochterski, R. L. Martin, K. Morokuma, V. G. Zakrzewski, G. A. Voth, P. Salvador, J. J. Dannenberg, S. Dapprich, A. D. Daniels, Ö. Farkas, J. B. Foresman, J. V. Ortiz, J. Cioslowski and D. J. Fox, *Gaussian 09*, Gaussian Inc., Wallingford, CT, 2009.
22 A. D. Becke, *J. Chem. Phys.*, 1993, **98**, 5648–5652.
23 For recent applications of these DFT theory levels to mechanistic studies, see: (*a*) G. Hirata and H. Maeda, *Org. Lett.*, 2018, **20**, 2853–2856; (*b*) J. P. Barham, S. E. Dalton, M. Allison, G. Nocera, A. Young, M. P. John, T. McGuire, S. Campos, T. Tuttle and J. A. Murphy, *J. Am. Chem. Soc.*, 2018, **140**, 11510–11518; (*c*) A. S.-K. Tsang, A. Kapat and F. Schoenebeck, *J. Am. Chem. Soc.*, 2016, **138**, 518–526; (*d*) M. Salamone, G. A. DiLabio and M. Bietti, *J. Org. Chem.*, 2011, **76**, 6264–6270; (*e*) X. Peng, B. M. K. Tong, H. Hirao and S. Chiba, *Angew. Chem., Int. Ed.*, 2014, **53**, 1959–1962.
24 Reactions with a 20 kcal mol^{-1} barrier proceed spontaneously at rt. At 25 °C, a fraction of 2.21×10^{-15} molecules have energies exceeding the activation energy according to the Boltzmann distribution. This translates to reactions with 33.4 kcal mol^{-1} barriers proceeding spontaneously at 80 °C.
25 Data points between at least the first 200–700 s of the reaction were used, depending on the reaction speed. At least 6 data points were used for fitting the initial rates. See ESI for details.†
26 See ref. 5 and ESI therein. Under ambient air/moisture a 20 mol% loading of KO*t*Bu gave almost no reaction of DMA (**1**) + styrene (1% **6**) yet a 60 mol% loading gave near-full conversion to products (71% **6**, 16% **10**), see ref. 5 (Table S2.1). To confirm that catalytic activity was enabled

by absence of ambient air/moisture and not by DMSO-d_6 cosolvent (Table 2, entry 7 herein), the reaction of styrene and DMA (**1**) using 25 mol% KO*t*Bu was repeated in absence of DMSO-d_6 and gave **6** (36%) and **10** (12%) upon quenching after 2 h. In presence of DMSO-d_6 cosolvent (Table 2, entry 7), the combined products **6** + **10** = *ca.* 83% after *ca.* 2 h based on the kinetic plot, see ESI.†

27 Hammett substituent coefficients were assumed based on the corresponding benzoic or naphthoic acids, see: D. H. McDaniel and H. C. Brown, *J. Org. Chem.*, 1958, **23**, 420–427.

28 This pattern was also observed for the C-alkylation of 2-alkylpyridines in ref. 4, where products '**3sa**' and '**3ta**' in that paper resulted from acyclic and cyclic substrates, respectively. Product '**3ta**' was obtained in higher yield at lower temperature than '**3sa**'.

29 Although these previously-reported[5] conditions in DMSO solvent (Fig. 8) differ slightly in styrene concentration and equivalents of amide, inviting the thought that greater equivalents of **21** could have given rise to higher B/M selectivity, in fact the reaction of styrene (0.45 M) in NMP solvent gave an identical B/M selectivity (Fig. 9). The similar B/M ratios for reactions with *vs.* without DMSO (Fig. 11) supports the conclusion that DMSO does not participate in the reaction mechanism.

30 E. M. Simmons and J. F. Hartwig, *Angew. Chem., Int. Ed.*, 2012, **51**, 3066–3072.

31 I. Sato, Y. Yamashita and S. Kobayashi, *Synthesis*, 2019, **51**, 240–250.

32 For an example study showing that an intermolecular competition cannot identify C-H cleavage as the turnover-limiting step, see: L. M. Geary and P. G. Hultin, *Eur. J. Org. Chem.*, 2010, 5563–5573.

33 For example studies appropriately selected to identify C–H cleavage as the turnover-limiting step, see: (*a*) H. Y. Sun, S. I. Gorelsky, D. R. Stuart, L.-C. Campeau and K. Fagnou, *J. Org. Chem.*, 2010, **75**, 8180–8189; (*b*) Ref. 4.

34 The NMP-d_9 supplier's specification of D-incorporation at 99% can account for the 0.8% relative abundance of **20a-d_6** but cannot account for the entire 2.3% relative abundance of **20a-d_8**, which must therefore form under the reaction conditions and may be rationalized by adventitious water present in reagents/solvents/KO*t*Bu. Total water content in NMP-d_9 was determined at 3400 ppm (Karl Fischer) by the supplier.

35 While D-incorporation at the benzylic position from DMSO-d_6 solvent cannot be completely ruled out in Fig. 11B reactions, the NMR spectrum over time showed signals consistent with **20a-h_{18}** only (see ESI†). Benzylic D-incorporation observed in Fig. 11A reactions strongly implicates the NMP-d_9 as the source of D.

36 The ionization behavior of all deuterated analogues of **20a** was assumed to be identical, given their structural similarity.

37 J. P. Barham, G. Coulthard, R. G. Kane, N. Delgado, M. P. John and J. A. Murphy, *Angew. Chem., Int. Ed.*, 2016, **55**, 4492–4496.

38 To confirm catalytic activity was enabled by absence of ambient air/moisture and not by DMSO-d_6 cosolvent (Table 3, entry 3), the reaction of styrene and NMP (**19**) using 25 mol% KO*t*Bu was repeated in absence of DMSO-d_6 and gave **20a** (50%) and 10 (3%) upon quenching after 1 h. In presence of DMSO-d_6 cosolvent (Table 3, entry 3), the combined products **20a** + **20b** = *ca.* 100% after *ca.* 1 h based on the kinetic plot, see ESI.†

39 (*a*) G. Moad, E. Rizzardo and D. H. Solomon, *Macromolecules*, 1982, **15**, 909–914; (*b*) M. Nakajima, Q. Lefebvre and M. Rueping, *Chem. Commun.*, 2014, **50**, 3619–3622.

40 For previous reports regarding 18-crown-6 increasing reactivity by complexing potassium cations to generate a more reactive "naked" anion, or insights into the 18-crown-6/KO*t*Bu complex, see: (*a*) C. L. Liotta and H. P. Harris, *J. Am. Chem. Soc.*, 1974, **96**, 2250–2252; (*b*) F. L. Cook, C. W. Bowers and C. L. Liotta, *J. Org. Chem.*, 1974, **39**, 3416–3418; (*c*) S. Alunni, E. Baciocchi and P. Perucci, *J. Org. Chem.*, 1976, **41**, 2636–2638; (*d*) C. Kleeberg, *Z. Anorg. Allg. Chem.*, 2011, **637**, 1790–1794.

41 (*a*) V. P. Solov'ev, N. N. Strakhova, O. A. Raevsky, V. Rudiger and H.-J. Schneider, *J. Org. Chem.*, 1996, **61**, 5221–5226; (*b*) G. Wipff, P. Weiner and P. Kollman, *J. Am. Chem. Soc.*, 1982, **104**, 3249–3258.

42 Y. Yamashita, K. Minami and S. Kobayashi, *Chem. Lett.*, 2018, **47**, 690–692.

43 (*a*) B. G. Chatterjee, R. F. Abdulla and N. L. Nyss, *Z. Naturforsch., B: J. Chem. Sci.*, 2014, **8**, 771–773; (*b*) P. Venturello and M. Barbero, *Sci. Synth.*, 2006, **8**, 1361–1364.

44 For examples of dimsyl anion generation when DMSO is treated with NaO*t*Bu/KO*t*Bu, see: (*a*) O. Bortolini, G. Fantin, V. Ferretti, M. Fogagnolo, P. P. Giovannini, A. Massi, S. Pacifico and D. Ragno, *Adv. Synth. Catal.*, 2013, **355**, 3244–3252; (*b*) J. P. Barham, G. Coulthard, K. E. Emery, E. Doni, F. Cumine, G. Nocera, M. P. John, L. E. A. Berlouis, T. McGuire, T. Tuttle and J. A. Murphy, *J. Am. Chem. Soc.*, 2016, **138**, 7402–7410; (*c*) M. E. Budén, J. I. Bardagí, M. Puiatti and R. A. Rossi, *J. Org. Chem.*, 2017, **82**, 8325–8333.

45 In ref. 3, cyclohexanone gave a '6–11%' yield of bisadduct; the mean average yield (9%) was assumed for this study.

46 Isolated yields of **26a**/**26b** and **28a**/**28b** suffered somewhat due to failure of column chromatography to separate monoadducts from bisadducts and the requirement for multiple GPC purifications. The NMR yields of **26a** and **26b** could not be determined due to overlapping peaks in the NMR spectrum of crude products; but analysis of the mass spectra of crude reaction products supported the conclusion of a lower B/M ratio in the reaction of **27**, see ESI.†

47 F. G. Bordwell and J. A. Harrelson Jr., *Can. J. Chem.*, 1990, **68**, 1714–1718.

48 A recent report, ref. 31, showed successful addition of potassium benzylate species (generated from alkylarenes by KCH_2TMS) to stilbenes and vinylsilanes, but unsuccessful

addition to styrenes. Based on the mechanism identified herein for analogous reactions, the co-ordinating heteroatom setting up the metal–ene transition state is unnecessary for reactivity (due to the likely small pK_a difference between the initial and final potassium benzylates) but its absence presumably decreases stability of the formed potassium benzylate and promotes oligomerization.

49 W. Oppolzer, *Angew. Chem., Int. Ed. Engl.*, 1989, **28**, 38–52.

50 H. Lehmkuhl and D. Reinehr, *J. Organomet. Chem.*, 1970, **25**, C47–C50.

51 Selected examples: (*a*) W. Oppolzer and K. Bättig, *Tetrahedron Lett.*, 1982, **23**, 4669–4672; (*b*) W. Oppolzer and A. F. Cunningham, *Tetrahedron Lett.*, 1986, **27**, 5467–5470.

52 Y.-F. Liu, L. Zheng, D.-D. Zhai, X.-Y. Zhang and B.-T. Guan, *Org. Lett.*, 2019, **21**, 5351–5356.